

This item is the archived peer-reviewed author-version of:

NiO-nanoparticles induce reduced phytotoxic hazards in wheat (*Triticum aestivum* L.) grown under future climate CO_2

Reference:

Saleh Ahmed M., Hassan Yasser M., Selim Samy, Abd Elgawad Hamada.- NiO-nanoparticles induce reduced phytotoxic hazards in wheat (*Triticum aestivum* L.) grown under future climate CO_2
Chemosphere - ISSN 0045-6535 - 220(2019), p. 1047-1057
Full text (Publisher's DOI): <https://doi.org/10.1016/J.CHEMOSPHERE.2019.01.023>
To cite this reference: <https://hdl.handle.net/10067/1574610151162165141>

Accepted Manuscript

NiO-nanoparticles induce reduced phytotoxic hazards in wheat (*Triticum aestivum* L.) grown under future climate CO₂

Ahmed M. Saleh, Yasser M. Hassan, Samy Selim, Hamada AbdElgawad



PII: S0045-6535(19)30024-4

DOI: <https://doi.org/10.1016/j.chemosphere.2019.01.023>

Reference: CHEM 22938

To appear in: *ECSN*

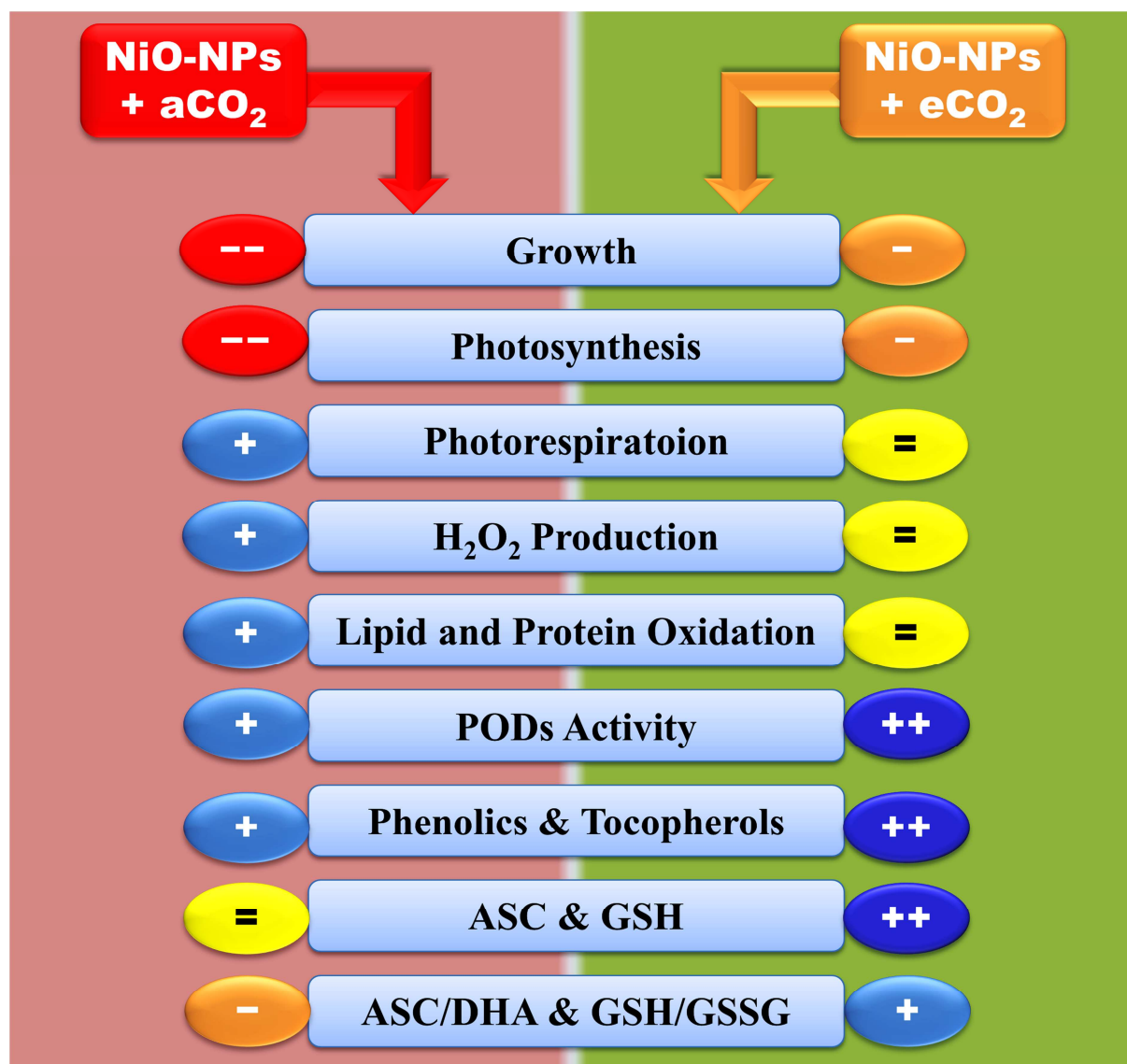
Received Date: 5 October 2018

Revised Date: 13 December 2018

Accepted Date: 3 January 2019

Please cite this article as: Saleh, A.M., Hassan, Y.M., Selim, S., AbdElgawad, H., NiO-nanoparticles induce reduced phytotoxic hazards in wheat (*Triticum aestivum* L.) grown under future climate CO₂, *Chemosphere* (2019), doi: <https://doi.org/10.1016/j.chemosphere.2019.01.023>.

This is a PDF file of an unedited manuscript that has been accepted for publication. As a service to our customers we are providing this early version of the manuscript. The manuscript will undergo copyediting, typesetting, and review of the resulting proof before it is published in its final form. Please note that during the production process errors may be discovered which could affect the content, and all legal disclaimers that apply to the journal pertain.



**NiO-nanoparticles induce reduced phytotoxic hazards in wheat
(*Triticum aestivum* L.) grown under future climate CO₂**

Ahmed M. Saleh^{1,2,*}, Yasser M. Hassan³, Samy Selim^{4,5}, Hamada Abdelgawad^{3,6*,a}

¹Biology Department, Faculty of Science at Yanbu, Taibah University, King Khalid Rd., Al Amoedi, 46423 Yanbu El-Bahr, Saudi Arabia.

²Department of Botany and Microbiology, Faculty of Science, Cairo University, Giza 12613, Egypt.

³Department of Botany and Microbiology, Faculty of Science, Beni-Suef University, 62521 Beni-Suef, Egypt.

⁴Department of Clinical Laboratory Sciences, College of Applied Medical Sciences, Jouf University, Sakaka, P.O. 2014, Saudi Arabia.

⁵Botany Department, Faculty of Science, Suez Canal University, Ismailia, P.O. 41522, Egypt.

⁶Laboratory for Molecular Plant Physiology and Biotechnology, Department of Biology, University of Antwerp, Groenenborgerlaan 171, B-2020, Antwerp 2020, Belgium.

^aThese authors contributed equally to this manuscript.

***Corresponding Authors**

A. M. Saleh, Email: asaleh@sci.cu.edu.eg, Phone: +966 54 116 1474

H. Abdelgawad, Email: hamada.abdelgawad@uantwerpen.be, Phone: +32(0)32653826,

Running title:

eCO₂ mitigates NiO-NPs-induced oxidative stress in wheat

Keywords

CO₂; NiO nanoparticles; Photosynthesis; Photorespiration; Antioxidants; Glutathione; Ascorbate

1 Abstract

2 Due to industrialization and expansion of nanotechnology, ecosystem contamination by
3 nanoparticles is likely. Overall, nanoparticles accumulate in environmental matrices and induce
4 phytotoxicity, however future climate (elevated CO₂ (eCO₂)) may affect the distribution of
5 nanoparticles in ecosystems and alter their impact on plants. In the current study, nickel oxide
6 nanoparticles (NiO-NPs) with an average diameter of 54 nm were synthesized using Triton X-
7 100 and characterized by scanning electron microscopy (SEM), UV-VIS spectroscopy and
8 Fourier transform infrared spectroscopy (FTIR). We have investigated the impact of NiO-NPs at
9 a concentration of 120 mg kg⁻¹ soil, selected based on the results of a preliminary experiment, on
10 accumulation of Ni ions in wheat (*Triticum aestivum* L.) and how that could influence plant
11 growth, photosynthesis and redox hemostats under two CO₂ scenarios, ambient (aCO₂, 400 ppm)
12 and eCO₂ (620 ppm). NiO-NPs alone reduced whole plant growth, inhibited photosynthesis and
13 increased the levels of antioxidants. However, improved defense system was not enough to
14 lessen photorespiration induced H₂O₂ accumulation and oxidative damage (lipid and protein
15 oxidation). Interestingly, eCO₂ significantly mitigated the phytotoxicity of NiO-NPs. Although,
16 eCO₂ did not affect Ni accumulation and translocation in wheat, it promoted photosynthesis and
17 inhibited photorespiration, resulting in reduced ROS production. Moreover, it further improved
18 the antioxidant defense system and maintained ASC/DHA and GSH/GSSG redox balances.
19 Organ specific responses to NiO-NPs and/or eCO₂ were indicated and confirmed by cluster
20 analysis. Overall, we suggest that wheat plants will be more tolerant to NiO-NPs stress under
21 future climate CO₂.

23 1. Introduction

24 Over the last decades, there has been a growing advance of consumer products based on
25 nano-sized heavy metal. For instance, due to its unique properties, nano-sized nickel oxide (NiO-
26 NPs) is utilized for several products, such as batteries, gas sensors and electrochromic devices
27 (Kim and Lee, 2014; Salimi et al., 2007; Zhu et al., 2012). Inevitably, these nano-sized heavy
28 metals are likely released both from point and nonpoint sources leading to deterioration of
29 environmental matrices and toxification of biota (Nowack and Bucheli, 2007). In fact, because of
30 their higher dissolution, nano-sized heavy metals represent a stronger environmental hazard, as
31 compared with their bulk form (Faisal et al., 2013; Katsumiti et al., 2016). Therefore, risk
32 assessment and amelioration of biological toxicity of nano-sized heavy metals have received
33 much attention (Savolainen et al., 2010; Torabifard et al., 2018). In this regard, many
34 investigations have addressed the toxicological behavior of nano-sized heavy metals on animals,
35 however much less efforts have been devoted for their phytotoxicity (Meena et al., 2015; Sager
36 et al., 2016). Beside their importance in sustenance of food for human, plants are essential
37 component of the ecosystem and are frequently subjected to environmental pollutants, such as
38 nano-sized heavy metal (Antisari et al., 2015). Therefore, substantial efforts should be given to
39 develop efficient approaches for alleviating the impact of such pollutants on plant productivity
40 and limiting their accumulation in the edible parts of the plant.

41 Despite of the considerable difference in their physical properties, once inside plants
42 nano-sized heavy metals impose the same toxicological mechanisms as their bulk form (Faisal et
43 al., 2013; Soares et al., 2018; Yusuf et al., 2011). It is well recognized that Ni is an essential
44 micronutrient for plants, it is utilized as a cofactor for several metalloenzymes such as urease and
45 glyoxalase I (Brown et al., 1987). However, at higher concentrations of Ni, 10 mg/Kg dry mass

46 in sensitive species, phytotoxicity symptoms such as chlorosis, necrosis and wilting are evident
47 (Yusuf et al., 2011). The deleterious effect of Ni on plant growth, could be ascribed to its
48 negative impact on photosynthesis, dark respiration and mineral nutrition (Seregin and
49 Kozhevnikova, 2006; Srivastava et al., 2012). By considering its impact on photosynthesis, Ni
50 has been reported to inhibit the synthesis of photosynthetic pigments, replace the Mg ion of
51 chlorophyll molecule, induce damage in the thylakoid membrane, restrain electron transport
52 chain, and inhibit the activity of ribulose-1,5-biphosphate carboxylase/oxygenase (rubisco) and
53 other Calvin cycle enzymes (Soares et al., 2016; Srivastava et al., 2012; Yusuf et al., 2011).
54 Owing to its critical role in metabolism, such suppression of the photosynthetic C assimilation is
55 inevitably reflected on other metabolic processes as well as plant growth and development.
56 Although Ni is not a redox active metal, but it is known to impose oxidative stress, mainly
57 through impairing redox homeostasis leading to accumulation of reactive oxygen species (ROS)
58 that is normally produced during metabolic processes (Baccouch et al., 2006; Pandey and Gopal,
59 2010). Under these circumstances, the increased levels of ROS can result in damage of cell
60 compartments, by oxidation of lipids and proteins, and disturbance of cellular functions (Apel
61 and Hirt, 2004). Therefore, to tolerate the toxic levels of Ni, plants have to develop an efficient
62 antioxidant defense system and to maintain proper performance of the critical physiological
63 processes, such as photosynthesis.

64 Unlike its bulk counterpart, limited number of studies have addressed the stress imposed
65 by nano-sized Ni, e.g. NiO-NPs, on plants. In this regard, Faisal et al. (2013) assessed the
66 phytotoxicity of NiO-NPs using roots of tomato seedlings as an *in vivo* model. They reported that
67 NiO-NPs treatment reduced root elongation, increased the levels of ROS, lipid peroxidation,
68 glutathione (GSH) and superoxide dismutase (SOD) activities, and induced cell death as

69 indicated by the increased number of apoptotic and necrotic cells. They ascribed the oxidative
70 damage caused by NiO-NPs to dissolution, uptake and accumulation of Ni ions in the plant
71 tissues, which was significantly higher as compared to the bulk form of NiO. Recently,
72 cultivation of barley in artificial soil treated with NiO-NPs (120 mg kg⁻¹) resulted in significant
73 reduction in growth and photosynthesis related parameters (Soares et al., 2018). They found that
74 NiO-NPs triggered oxidative damage in barley, as revealed by overproduction of ROS and
75 higher lipid peroxidation.

76 Another factor that represents a future challenge for plants is the progressive increase in
77 the concentration of atmospheric CO₂ (IPCC, 2013). Interestingly, within a physiological range,
78 elevated CO₂ (eCO₂) has been reported to improve plant growth by enhancement of the
79 photosynthetic C assimilation; thus providing the building blocks and energy required for plant
80 growth and development (Misra and Chen, 2015; Tuba et al., 2003; Watanabe et al., 2014).
81 Moreover, it has been documented that eCO₂ could mitigate the adverse effect exerted by various
82 stress factors on plants (Abdelgawad et al., 2016; Pérez-López et al., 2009; Zinta et al., 2014).
83 eCO₂ could not only affect plant growth and physiology, but it may also alter the distribution of
84 contaminants, such as heavy metals, in the ecosystem. In this regard, some investigations have
85 addressed the impact of elevated CO₂ on the uptake, accumulation and partitioning of some
86 heavy metals in hyperaccumulator and nonaccumulator plant species (Guo et al., 2011; Li et al.,
87 2010). In addition, some efforts has been devoted to study the combined effect of eCO₂ and
88 limited number of heavy metal (Cd, Cu and to less extent Pb) on growth, photosynthesis and
89 some parameters related to the antioxidant defense systems in hyperaccumulator plants (Guo et
90 al., 2015; Jia et al., 2010; Pietrini et al., 2016). On contrary, much less attention has been given
91 for the effect of eCO₂ on the phytotoxicity induced by nano-sized heavy metals. In this context,

92 eCO₂ was reported to intensify the adverse effect of TiO₂-NPs on growth of rice and wheat by
93 improving the uptake and translocation of Ti (Du et al., 2017; Jiang et al., 2017). Moreover,
94 Yadav et al. (2014) found that eCO₂ treatment improved the accumulation of Fe and Zn in
95 different parts of rice plant grown in hydroponic cultures supplemented with different
96 concentrations of Fe₂O₃-NPs and ZnO-NPs, respectively. However, none of these studies had
97 investigated the impact of eCO₂ on the antioxidant defense system of plants under nano-sized
98 heavy metal contamination. Moreover, so far there are no studies investigating the concurrent
99 effect of nano-sized Ni and eCO₂ on plants

100 In the current study, we have addressed the impact of NiO-NPs, alone or in combination
101 with future climate CO₂, on growth and redox homeostasis in one of the most important crops for
102 human food, bread wheat (*Triticum aestivum* L.). The uptake and accumulation of Ni ions and
103 the triggered changes in photosynthesis, photorespiration, molecular ROS scavengers and
104 antioxidant enzymes as well as the detailed changes in ASC-GSH cycle were studied in wheat
105 subjected to NiO-NPs (120 mg/Kg soil) under two levels of CO₂, ambient (aCO₂, 400 ppm) and
106 eCO₂ (620 ppm).

107

108 **2. Materials and methods**

109 *2.1. Preparation of Nickel oxide nanoparticles (NiO-NPs)*

110 NiO-NPs were synthesized following the method adopted by Kooti and Jorfi (2009). To
111 200 ml of $\text{NiCl}_2 \cdot 6\text{H}_2\text{O}$ (0.1 M), 5ml of Triton X-100 was added and the solution was stirred for
112 15 min. Then, 200ml of sodium hypochlorite solution containing 0.1M of NaOH was added
113 drop wise under continuous stirring for 20 min. The black precipitate of NiO_2 was performed at
114 6000 rpm for 10 min, then washed with distilled water. The collected precipitate was placed into
115 a beaker containing 50 mL of methanol and stirred for 2 h till the black solid turned to dark olive
116 green indicating the formation of NiO. The green precipitate was collected by centrifugation and
117 washed with distilled water and methanol and then dried in an oven at 90°C for 5 h, then
118 calcined at 300°C for 6h to afford nanosized NiO.

119 *2.2. Characterization of NiO-NPs*

120 *2.2.1. Size and morphology*

121 The size and morphology of synthesized NiO-NPs powder were characterized using
122 JEOL, JSM-6510 scanning electron microscope (SEM). The instrument was operated at 30 keV
123 and scanning electron imaging was taken with a resolution of 50,000 and a width of 250 mm on
124 a $0.5 \mu\text{m}$ scale.

125 *2.2.2. Ultraviolet-Visible Spectroscopy (UV-VIS)*

126 The optical features of NiO-NPs were determined on PE-UV Lambda 950 UV/VIS/NIR
127 in the wavelength range of 250-800 nm. NiO-NPs powders were suspended in
128 Dimethylformamide (DMF) with the help of a magnetic stirrer for 30 min prior analysis by UV-
129 VIS spectrophotometer.

130 *2.2.3. Fourier transform infrared spectroscopy (FTIR)*

131 FTIR analysis of NiO-NPs powder was performed using a Bruker IFS66V
132 FTIR spectrometer for the frequency range between 4000 and 400 cm^{-1} at room
133 temperature. NiO sample was mixed with potassium bromide, which were ground and pressed
134 into a transparent pellet with a diameter of 13 mm.

135 2.3. *Experimental setup*

136 Uniform wheat seeds (*Triticum aestivum* L., Sids 13, a commercial variety) were surface
137 sterilized with 35 % (v/v) of commercial bleach for 30 min. Sterilized seeds were grown in pots
138 contained artificial soil with 5% organic matter and pH 6 (OECD, 2006). Pots were transferred
139 to controlled-growth rooms under varied climate conditions, viz: 1) ambient CO_2 (aCO_2) (400
140 ppm), 2) aCO_2 + NiO-NPs (120 mg/Kg soil), 3) elevated CO_2 (eCO_2) (620 ppm), 4) eCO_2 +
141 NiO-NPs (120 mg/Kg soil). NiO-NPs were applied after 1 week from sowing in the form of
142 suspension. Other climate conditions included: light intensity of 150 $\mu\text{mol m}^{-2} \text{s}^{-1}$, 16/8 h
143 day/night photoperiod, 21/18 °C air temperature and 60/70% humidity. After 3 weeks of NiO-
144 NPs exposure, roots and leaves were harvested. Harvested materials were immediately frozen in
145 liquid N_2 , and stored at -80 °C for biochemical analysis. The concentration of NiO-NPs was
146 chosen based on the results of preliminary assays on the impact of a range of NiO-NPs doses
147 (60-480 mg/Kg soil) on growth and accumulation of stress markers in wheat plants, under both
148 aCO_2 and eCO_2 (supplementary materials).

149 2.4. *Determination of photosynthesis rate and stomatal conductance*

150 For measuring the rates of photosynthesis and stomatal conductance the protocols
151 described in our previous work (Al Jaouni et al., 2018) were followed up. Photosynthesis at
152 saturating light (Asat , $\mu\text{mol CO}_2 \text{m}^{-2} \text{s}^{-1}$) were determined (LI-COR LI-6400, LI-COR Inc.,
153 Lincoln, NE, USA) on the youngest fully expanded. A minimum of 5 min of leaf equilibration

154 was set at each step before data were logged. LI-COR leaf chamber conditions were set at 400 or
155 620 ppm CO₂, 22 °C (block temperature) and saturated photon flux density (1500 μmol m⁻² s⁻¹).
156 Stomatal conductance (gs, mol CO₂ m⁻² s⁻¹) was measured on the abaxial side of
157 fully developed leaves with a Leaf Porometer (Model SC-1, Decagon Devices, Inc., Hopkins,
158 Pullman, WA USA). The average vapor pressure deficit and leaf temperature were 0.37±0.02
159 and 20±2.02, respectively. Chlorophyll fluorescence was measured on dark acclimated fully
160 expanded leaves using FMS-2 pulse-modulated fluorometer (Hansatech Instruments, Norfolk,
161 UK). The minimal fluorescence (F₀) and maximal fluorescence (F_m) were measured for 30
162 min dark-adapted leaves. The photochemical efficiency of PSII (F_v/F_m) for dark adapted leaves
163 were calculated, where F_v (Maximal variable fluorescence) = F_m - F₀.

164 2.5. Photorespiration

165 Glycolate oxidase (GO) and hydroxypyruvate reductase (HPR) activities were measured
166 according to (Feierabend and Beevers, 1972; Schwitzguebel and Siegenthaler, 1984),
167 respectively. Moreover, to calculate glycine/serine ratio, frequently used as an index to estimate
168 photorespiration (Kebeish et al., 2007), glycine and serine were quantified using a Waters
169 Acquity UPLC-tqd system (Al Jaouni et al., 2018).

170 2.6. Stress markers

171 Lipid peroxidation was determined according to the thiobarbituric acid assay (Hodges et
172 al., 1999). Protein oxidation was assessed via carbonyl quantification (Levine et al., 1994).
173 Xylenol orange method was employed to quantify Hydrogen peroxide (H₂O₂) in TCA (0.1%)
174 extract of plant samples (Murphy and Noack, 1994). The concentration of nitric oxide was
175 determined by measuring the production of methemoglobin (Feelisch and Noack, 1987).

176 *2.7. Total antioxidant capacity (TAC)*

177 TAC was assessed according to the FRAP (ferric reducing antioxidant power) method
178 described by Benzie and Strain (1999) using trolox (Sigma-Aldrich, St. Louis, MO, USA) as a
179 standard.

180 *2.8. Triphenyltetrazolium chloride–dehydrogenase activity (TTC-DHA) assay*

181 The activity of dehydrogenase was measured by TTC reduction method (Casida Jr et al.,
182 1964). Samples were treated with 0.1 M TTC and incubated for 24 h at 37°C. Formed triphenyl
183 formazan was extracted and assayed at 485 nm. *TTC-DHA* was expressed as μg formazan/g
184 tissue

185 *2.9. Antioxidant metabolites*

186 Reduced ascorbate (ASC) and reduced glutathione (GSH) were quantified by HPLC.
187 Total ascorbate (ASC+DHA) and glutathione (GSH+GSSG) concentrations were determined
188 after reduction with DTT as described in Zinta et al. (2014). Polyphenols and flavonoids were
189 quantified using Folin-Ciocalteu and aluminum chloride assays, respectively (Mohamed et al.,
190 2017). Separation and quantification of tocopherols were conducted by HPLC (Shimadzu,
191 Hertogenbosch, Netherlands) using normal phase conditions (Particil Pac 5 μm column mate-
192 rial, length 250 mm, i.d. 4.6 mm).

193 *2.10. Antioxidant enzyme activities*

194 Superoxide dismutase (SOD), peroxidase (POD), catalase (CAT), glutathione peroxidase
195 (GPX), ascorbate peroxidase (APX), glutathione reductase (GR), monodehydroascorbate
196 reductase (MDHAR), dehydroascorbate reductase (DHAR), glutathione-S-transferase (GST)
197 activities were assayed according to the protocols described in our previous work (Abdelgawad
198 et al., 2015).

199 *2.11. Statistical analyses*

200 Data analyses were performed using the procedures provided in Statistical Analysis
201 System (SPSS Inc., Chicago, IL, USA). Data normality and the homogeneity of variances were
202 checked using the KolmogoroveSmirnov test and Levene's test, respectively. All the data were
203 subjected to one-way Analysis of Variance (ANOVA). Tukey's Test ($p < 0.05$) was carried out
204 as the post-hoc test for mean separations. Number of replicates for each experiment were three (n
205 = 3). Cluster analysis was performed by using Pearson distance metric of the MultiExperiment
206 Viewer (MeV)TM 4 software package (version 4.5, Dana-Farber Cancer Institute, Boston, MA,
207 USA).

208 **3. Results**

209 *3.1. Characterization of NiO-NPs*

210 The size and morphology of the synthesized NiO-NPs is shown in Figure 1a. SEM image
211 revealed that, particles are homogeneous shaped particles with an average size of 54 nm.
212 Additionally, the image shows that, the synthesized particles have a tendency to form uniform
213 aggregations, therefore, uniform particle dimension (shape and size). UV-VIS analysis (Figure
214 1b) displays that, NiO nanoparticles exhibit the characteristic absorption edge in the range of
215 280-350 nm. From FTIR spectrum of fabricated NiO nanoparticles (Figure 1c), the peak at
216 3418.1 cm^{-1} is ascribed to O-H group stretching vibrational mode and the peak at 1625.48 cm^{-1} is
217 attributed to the bending vibrational mode of O-H group. The appearance of these peaks
218 indicated the presence of water molecules trapped on the surface of NiO particles from
219 surrounding atmosphere. Additionally, there is band absorption in the range of $424.38\text{--}542.18$
220 cm^{-1} , corresponding to the Ni-O bond stretching vibration, while, absorption band at 636 cm^{-1} is
221 assigned to Ni-O-H stretching bond.

222 *3.2. Ni accumulation and biomass production*

223 plants grown under eCO₂ have significantly higher biomass than those grown in aCO₂
224 (Table 1). NiO-NPs reduced biomass production under both levels of CO₂. However, the NiO-
225 NPs-induced biomasses reduction was much lower under eCO₂ than under. Root growth was
226 more affected by NiO-NPs than shoot, whereas about 52% and 41% inhibition in dry masses
227 were observed for root and shoot, respectively. On the other hand, NiO-NPs increased Ni ions
228 accumulation in root and shoot at both CO₂ levels. Meanwhile, the concentration of Ni ions in
229 both organs was not significantly affected by CO₂ enrichment.

230 *3.3. Photosynthesis and stomatal conductance*

231 Elevated CO₂ alone did not significantly affect chlorophyll and carotenoids contents,
232 chlorophyll fluorescence, rubisco activity or stomatal conductance; however it significantly
233 improved the net photosynthetic rate and consequently increased starch level (Table 2). On the
234 other hand, NiO-NPs significantly decreased all photosynthesis related parameters, except for the
235 content of carotenoids that was significantly increased. Interestingly, the synchronous treatment
236 with eCO₂ and NiO-NPs significantly mitigated NiO-NPs-induced inhibition in photosynthesis
237 related parameters . The values of photosynthesis related parameters, except for carotenoids,
238 under the combined treatment (eCO₂+NiO-NPs) were significantly higher than those in NiO-NPs
239 alone treatment (Table 2).

240 *3.4. Photorespiration*

241 As compared with the control plants, eCO₂ had no significant impact on photorespiratory
242 key enzymes (GO or HPR) as well as the glycine/serine ratio; while NiO-NPs significantly
243 induced them (Table 2). Interestingly, the co-application of eCO₂ with NiO-NPs significantly
244 reduced the impact of NiO-NPs on photorespiration related parameters.

245 *3.5. Stress markers, TAC and TTC-DHA*

246 Atmospheric enrichment with eCO₂ had no significant effect on the levels of H₂O₂,
247 MDA, NO or protein carbonyls in either root or shoot tissues (Figure 2). On contrary, NiO-NPs
248 treatment significantly increased H₂O₂ and MDA levels in root and shoot and protein carbonyls
249 and NO level in root of aCO₂ treated plants. The coexistence of eCO₂ and NiO-NPs significantly
250 reduced the levels of the measured oxidative markers to values comparable to those detected in
251 the control plant.

252 Although, TAC or TTC-DHA levels were not altered in eCO₂ treated plants, they were
253 scientifically reduced in shoot and root after NiO-NPs treatment (Figure 2). Meanwhile, the
254 incorporation of eCO₂ mitigated the NiO-NPs-induced inhibition in TTC-DHA, which was in
255 consistence with the improvement in TAC (FRAP) in root and to less extent in shoot.

256 3.6. Antioxidant metabolites

257 Phenolics, flavonoids and tocopherols levels were not significantly affected by eCO₂
258 treatment (Figure 2). NiO-NPs treatment alone improved the accumulation of these antioxidants
259 in root but not in shoot tissues. CO₂ enrichment further improved the levels of tocopherols in
260 root and that for phenolics in shoot of NiO-NPs treated plant, while it had no significant impact
261 on the content of flavonoids.

262 3.7. SOD, CAT, POD and GST activities

263 CO₂ enrichment had no significant impact on SOD, CAT and POD activities (Figure 2).
264 Plant treated with NiO-NPs showed increase in POD activity in both organs, but not in SOD
265 activity, relative to the control plant. On the other hand, CAT activity significantly increased
266 only in root-treated with NiO-NPs and eCO₂. No change in GST activity was observed for shoot
267 after eCO₂ and/or NiO-NPs treatments, while it was significantly improved in root of NiO-NPs
268 treated plant regardless of CO₂ level, whereas the improvement was more evident in the
269 combined treatment.

270 3.8. ASC-GSH cycle

271 GSH/ASC cycle related enzymes and metabolites were not altered by eCO₂ treatment in
272 root (Figure 2). However, eCO₂ treatment caused significant improvement in the MDAR activity

273 and in the ratios of ASC/DHA and GSH/GSSG in shoot, which was in consequence with reduced
274 levels of DHA and GSSG, respectively, rather than the increase in the concentrations of their
275 reduced forms, compared to control plant.

276 Regardless of the plant organ, NiO-NPs treatment improved GPX and GR activities, but
277 not APX, MDAR or DHAR activities. Moreover, NiO-NPs treatment increased the contents of
278 DHA in root and GSSG in both organs resulting in lower ASC/DHA and GSH/GSSG ratios in
279 plant grown under aCO₂. On the other hand, the synchronous existence of NiO-NPs and eCO₂
280 resulted in significant enhancement in GR and DHAR activities in root and shoot and that for
281 GPX and APX in root only, as compared with NiO-NPs alone treatment. Moreover, the
282 combined treatment (NiO-NPs+eCO₂) significantly recovered the decrease in ASC/DHA and
283 GSH/GSSG ratios in both organs. Such improvement in ASC/DHA and GSH/GSSG ratios was
284 mainly in consistence with increased levels of the reduced forms, ASC and GSH.

285 4. Discussion

286 The current study was conducted to assess, for the first time, how the future climate
287 (eCO₂) could alter the growth retardation and oxidative damage induced by NiO-NPs in wheat.
288 Although few studies have addressed the concurrent effect of eCO₂ and nano-sized heavy metals
289 on plants (Guo et al., 2011; Li et al., 2010), none of them had investigated the physiological and
290 biochemical mechanisms underlying the mitigating effect of eCO₂ on heavy metal-induced
291 oxidative stress in plants. Therefore, the current results have been discussed in view of the
292 previous studies addressing the combined effect of eCO₂ and other types of oxidative stress
293 inducing agents such as the bulk counterpart of heavy metals.

294 *4.1. eCO₂ did not affect Ni accumulation, but reduced NiO-NPs induced growth inhibition in*
295 *wheat plants.*

296 As one of the essential micronutrient for plants, Ni is normally taken up by roots and then
297 translocated to shoot in extremely small amounts, not exceeding few micrograms per gram dry
298 mass in nonaccumulators (Yusuf et al., 2011). However, increasing the level of Ni in the growth
299 medium is known to increase the uptake and translocation of Ni in plants (Pandey and Gopal,
300 2010; Rodrigues et al., 2017). Compared to their bulk counterpart NiO-NPs are reported to
301 provide higher levels of dissolved Ni ions, and consequently could exhibit higher uptake and
302 accumulation in the plant tissues (Faisal et al., 2013). In the current study, application of NiO-
303 NPs into the soil caused manifold increases in the concentration of Ni in both root and shoot
304 tissues, about 410 and 78 fold respectively under aCO₂ environment (Table 1). This result
305 suggests that Ni is preferentially accumulated in root tissues, a mechanism whereby plants act to
306 tolerate Ni toxicity by limiting the translocation of Ni to the photosynthetic organs (Soares et al.,

307 2018). In line with the present result, Soares et al. (2018) reported that root of barley grown
308 under NiO-NPs had accumulated much higher Ni than shoot did. Similar behavior was recorded
309 for wheat and other plants treated with bulk Ni (Pandey and Gopal, 2010; Rodrigues et al., 2017;
310 Soares et al., 2016; Uruç Parlak, 2016).

311 The comparable levels of Ni that detected in plants grown under both levels of CO₂
312 suggest that eCO₂ had no impact on the processes of uptake and translocation of Ni in wheat. In
313 fact, no studies have discussed the accumulation of Ni in eCO₂ treated-plants, however the
314 uptake and accumulation of other heavy metals such as Cd, Cu, Pb, Ti, Zn, and Fe from their
315 nano-sized or bulk forms under eCO₂ have been previously reported (Du et al., 2017; Guo et al.,
316 2015, 2011, Jia et al., 2016b, 2010; Jiang et al., 2017; Yadav et al., 2014). Moreover, heavy
317 metal accumulation in eCO₂ treated-plants seems to be dependent on the plant species and the
318 metal studied (Guo et al., 2015, 2011; Jia et al., 2010). For instance, Cd accumulation increased
319 in wheat and rice plants (Guo et al., 2011), but not in poplars and willows (Guo et al., 2015)
320 under CO₂ enriched environment.

321 Despite of the considerable difference in their physical properties, nano-sized heavy
322 metals share the same phytotoxicity mechanisms as their bulk counterpart (Faisal et al., 2013;
323 Soares et al., 2018; Yusuf et al., 2011). It is well known that Ni has deleterious effect on various
324 critical processes for plant growth and development such as cell division, nutrient utilization and
325 photosynthesis (Seregin and Kozhevnikova, 2006; Srivastava et al., 2012). The accumulation of
326 Ni reported herein was concomitant with a great reduction in wheat growth (Table 1). Such
327 growth retardation could be attributed to the adverse impact of NiO-NPs on photosynthesis
328 related parameters (chlorophyll and starch contents, chlorophyll fluorescence, rubisco activity
329 and the net photosynthetic rate). In agreement, parallel reductions in growth and chlorophyll

330 concentration and fluorescence in plants exposed to NiO-NPs (Soares et al., 2018) or bulk Ni
331 (Pandey and Gopal, 2010; Pandolfini et al., 1992; Rodrigues et al., 2017; Soares et al., 2016;
332 Yusuf et al., 2011) were reported.

333 Synchronous application of eCO₂ significantly recovered the inhibitory impact of Ni on
334 photosynthesis related parameters (Table 2) and consequently improved wheat growth (Table 1).
335 This stress mitigation role could be explained by the bio-fertilization activity of eCO₂,
336 particularly in C₃ plants such as wheat. In this context, increasing the CO₂ concentration, within
337 a physiological limit, could improve C fixation and thus lead to higher availability of non-
338 structural carbohydrates that are needed for normal plant growth and metabolism (Al Jaouni et
339 al., 2018). In fact, there is no literature about the combined effect of eCO₂ and Ni stress on
340 plants, however there are evidence that eCO₂ could reduce the deleterious impact of other heavy
341 metals, especially Cd, on growth and photosynthesis of hyperaccumulator and nonaccumulator
342 plants (Jia et al., 2016a; Li et al., 2010). The protective effect of eCO₂ on plants suffering Cd
343 and/or Pb stress was attributed to enhanced chlorophyll content, intracellular CO₂ concentration
344 and net assimilation rate (Guo et al., 2015; Jia et al., 2016b, 2010). Oppositely, eCO₂ further
345 strengthen the inhibitory effect of TiO₂-NPs on growth of rice and wheat (Du et al., 2017; Jiang
346 et al., 2017).

347 *4.2. eCO₂ mitigated NiO-NPs-induced oxidative damage in wheat via reducing H₂O₂ production*

348 As the current results revealed, NiO-NPs treatment had increased the endogenous Ni
349 levels in wheat. Although Ni is not considered as a redox active metal, but at phytotoxic levels
350 Ni is known to cause oxidative stress by impairing redox homeostasis leading to accumulation of
351 ROS (Gajewska and Skłodowska, 2007). Such over accumulation of ROS could trigger damage

352 of cell compartments by oxidation of lipids and proteins (Baccouch et al., 2006; Pandey and
353 Gopal, 2010). Oxidative damage due to increased uptake and accumulation of Ni from both
354 nano-sized and bulk materials was reported in wheat and other plant species (Baccouch et al.,
355 2006; Faisal et al., 2013; Pandolfini et al., 1992; Soares et al., 2018; Yusuf et al., 2011). In
356 agreement, we found that NiO-NPs induced sever oxidative stress i.e., higher levels of H₂O₂,
357 oxidation products of lipids and proteins (MDA and protein carbonyls, respectively) and NO (a
358 signal molecule in stress response), and reduced values of TTC-DHA (indication for cell
359 metabolic activity, (Berridge et al., 2005)). Similar to our results, Faisal et al. (2013) and Soares
360 et al. (2018) reported increases in the levels of ROS and MDA in tomato and barley after
361 treatment with NiO-NPs.

362 Interestingly, the coexistence of eCO₂ with NiO-NPs significantly mitigates the Ni-
363 induced oxidative stress, whereas treated plants grown under eCO₂ showed less tissue damage
364 e.g., reduced H₂O₂, MDA, protein carbonyls and NO levels, and increased TTC-DHA. In this
365 context, eCO₂ treatment has been reported to ameliorate the oxidative damage imposed by Cd on
366 poplar, willow and *lolium* sp. as indicated by lower levels of MDA as compared with Cd-stressed
367 plants grown under aCO₂ (Guo et al., 2015; Jia et al., 2010). Moreover, eCO₂ was found to to
368 decrease the production of H₂O₂, MDA and protein carbonyls in plants suffering several types of
369 oxidative stress-inducing agents such as heat, drought, salinity and ozone (Abdelgawad et al.,
370 2016, 2015; Zinta et al., 2014).

371 The mitigating effect of eCO₂ can be partly explained by downregulation of the stress
372 induced-H₂O₂ generating process such as photorespiration as indicated by decreased Gly/Ser
373 ratio and GO and HPR activities. Although H₂O₂ is produced by several cellular activities such
374 as NADH oxidase, lipid oxidation and mitochondrial electron transport chain, however

375 photorespiration is considered as the major and fastest pathway for production of H₂O₂ (Costa et
376 al., 2010; Foryer and Noctor, 2000; Quan et al., 2008). The lower photorespiration and higher
377 photosynthesis rates as affected by eCO₂ could be attributed to the improvement in the
378 carboxylation rather than the oxygenation activity of rubisco (Al Jaouni et al., 2018). Decreased
379 GO and HPR and Gly/Ser ratio as indication for lower photorespiration were frequently seen in
380 eCO₂ (Abdelgawad et al., 2015; Zinta et al., 2014). Taking together, these results suggest a role
381 for eCO₂ in maintaining redox homeostasis in plants grown under Ni stress by reducing the
382 production of ROS.

383 *4.3. eCO₂ improved ROS detoxification system and maintained GSH/GSSG and ASC/DHA redox*
384 *balances in NiO-NPs stressed wheat.*

385 Plants have evolved different strategies to maintain the levels of ROS under control.
386 These include molecular antioxidant scavengers, such as carotenoids, tocopherols, phenolics,
387 flavonoids, ASC and GSH, and the antioxidant enzymes SOD, CAT and various peroxidases
388 (Blokhina et al., 2003). Among these, the ASC/GSH pathway is of immense importance for
389 scavenging H₂O₂ (Foyer and Noctor, 2009). Overall, we found that eCO₂ improved TAC in root
390 and to less extent in shoot of NiO-NPs treated wheat. Such impact was in consistence with the
391 positive impact of eCO₂ on the accumulation of tocopherols in root and that for phenolics in both
392 root and shoot, under NiO-NPs stress. Similar increases in the contents of tocopherols and
393 phenolics were reported in *Arabidopsis thaliana* subjected to eCO₂ under combined heat and
394 drought stress (Zinta et al., 2014). The enhanced accumulation of phenolics and vitamins in
395 eCO₂ treated plants could be ascribed to the increased availability of C and N intermediates and
396 metabolic energy required for their biosynthesis (Herms and Mattson, 1992). In this regard, the

397 regulatory effect of eCO₂ on C and N metabolism is well known (Al Jaouni et al., 2018; Noguchi
398 et al., 2015; Nunes-Nesi et al., 2010).

399 The improved activity of peroxidases (APX, GPX and POX) reported herein under eCO₂
400 climate suggests a significant role for direct H₂O₂ scavenging enzymes in detoxification of H₂O₂
401 in wheat subjected to Ni stress. Similarly, Gajewska et al. (2006) recorded four-fold
402 improvement in POX activity in shoot of wheat treated with 200 µM Ni. Moreover, the activity
403 of APX were significantly improved by eCO₂ treatment in willow grown in high Cd
404 contamination (Guo et al., 2015). On the other hand, SOD activity was not affected by NiO-NPs
405 and or eCO₂ treatment in either root or shoot. In disagreement, SOD was improved in tomato and
406 barley subjected to NiO-NPs (Faisal et al., 2013; Soares et al., 2018). Thus, the response of SOD
407 to NiO-NPs seems to be species dependent.

408 Elevated CO₂ treated-plants possessed much higher GSH/GSSG and ASC/DHA ratios
409 during NiO-NPs stress. Such improved redox status could be attributed to the enhanced activities
410 of GSH and ASC recycling enzymes, GR and MDAR respectively, under CO₂ enriched
411 environment. This result points to a role for the GSH/ASC cycle, upregulated by eCO₂, in
412 confrontation of the oxidative stress imposed by Ni in wheat. GSH and ASC levels and
413 GSH/GSSG and ASC/DHA ratios are known to be constitutively elevated in plants adapted to
414 oxidative stress induced by heavy metals and other agents (Foyer, 1993; Seth et al., 2012; Yadav,
415 2010). Similar to our results, Jia et al. (2010) reported higher GSH levels in Cd-stressed *Lolium*
416 plants grown under eCO₂ compared to those grown in aCO₂. eCO₂ treatments also has been
417 found to enhance GR activity in willow plant exposed to Cd (Guo et al., 2015) and retrieve the
418 depletion in GSH/GSSG ratio caused by Cd in *Lemna minor* (Pietrini et al., 2016).

419 In fact, the enhanced GSH level is not only necessary for maintaining GSH/GSSG redox
420 balance and regeneration of ASC, as substrate for DHAR, but it is also important for
421 detoxification of heavy metals and xenobiotics, due to nucleophilic nature of its thiol group, in
422 a reaction catalyzed by GST (Yadav, 2010). Interestingly, the current result revealed that the
423 activity of GST was improved in wheat roots as affected by NiO-NPs, the effect that
424 strengthened by the co-application of eCO₂. In line with this result, Gajewska et al. (2006)
425 reported significant enhancement in GST activity in wheat in response to Ni treatment. Similar
426 improvement in GST activity was reported in *Pisum sativum* subjected to high concentrations of
427 Cd in hydroponic culture (Dixit et al., 2001).

428 4.4. Root and shoot respond differently to NiO-NPs under future eCO₂ climate

429 Hierarchical clustering of stress markers and antioxidant metabolites and enzymes in root
430 and shoot of wheat revealed variations in their response to NiO-NPs and/or eCO₂ treatments
431 (Figure 3). Overall, three major groups are distinguished: those were higher in shoot than in root
432 under eCO₂ levels, and were mainly improved in shoot of NiO-NPs treated plants by co-
433 application of eCO₂ (group 1); those were not affected by eCO₂ alone treatment in both organs,
434 but were improved in shoot and to more extent in root as affected by the combined treatment
435 (group 2); and those were improved in root only in response to NiO-NPs, regardless of CO₂ level
436 (group 3). Stress markers and most of direct H₂O₂ scavenging enzymes, were confined to group
437 3 and antioxidant metabolites were mainly clustered within group 2, while ASC-GSH cycle
438 related parameters were distributed all over the groups. The relatively higher accumulation of
439 H₂O₂, MDA, protein carbonyls and H₂O₂ detoxifying enzymes in roots of NiO-NPs treated
440 wheat indicates a severe oxidative damage in root than in shoot. Such effect could be ascribed to
441 the preferential accumulation of Ni ions in root, a mechanism whereby the plant act to limit the

442 translocation of Ni to the photosynthetic organs. Similarly, Soares et al. (2018) reported that root
443 of barley grown under NiO-NPs accumulated much higher Ni than shoot did. Moreover, Faisal et
444 al. (2013) reported that the accumulation of Ni ions in the roots of tomato seedlings treated with
445 NiO-NPs had resulted in severe oxidative damage as indicated by elevated levels of ROS and lipid
446 peroxidation products.

447 **5. Conclusion**

448 This study provides the first report regarding the interactive effect of NiO-NPs and eCO₂
449 on growth, photosynthesis, photorespiration and redox homeostasis in plants. Compared to NiO-
450 NPs alone, the co-application of eCO₂ improved growth and photosynthesis and mitigated Ni-
451 induced oxidative stress in wheat. In view of the present results, the plausible strategies whereby
452 eCO₂ mitigates the oxidative stress imposed by NiO-NPs in wheat include: (1) recovery of the
453 deleterious effect of Ni on photosynthesis; (2) Inhibition of photorespiration and therefore
454 decreasing the production of H₂O₂; (3) increasing ROS detoxification via improving antioxidant
455 defense. Consequently, reduced cellular damage (oxidized proteins and membrane lipids) and
456 proper GSH/GSSG and ASC/DHA redox balances (Figure 4) were observed in this study.

457 **Conflict of interest statement**

458 The authors declare that there are no conflicts of interest.

References

- Abdelgawad, H., Farfan-vignolo, E.R., Vos, D. De, Asard, H., 2015. Elevated CO₂ mitigates drought and temperature-induced oxidative stress differently in grasses and legumes. *Plant Sci.* 231, 1–10. doi:10.1016/j.plantsci.2014.11.001
- Abdelgawad, H., Zinta, G., Beemster, G.T.S., Janssens, I.A., 2016. Future climate CO₂ levels mitigate stress impact on plants : Increased defense or decreased challenge? *Front. Plant Sci.* 7, 1–7.
- Al Jaouni, S., Saleh, A.M., Wadaan, M.A.M., Hozzein, W.N., Selim, S., Abdelgawad, H., 2018. Elevated CO₂ induces a global metabolic change in basil (*Ocimum basilicum* L.) and peppermint (*Mentha piperita* L.) and improves their biological activity. *J. Plant Physiol.* 224–225, 121–131.
- Antisari, L.V., Carbone, S., Gatti, A., Vianello, G., Nannipieri, P., 2015. Uptake and translocation of metals and nutrients in tomato grown in soil polluted with metal oxide (CeO₂, Fe₃O₄, SnO₂, TiO₂) or metallic (Ag, Co, Ni) engineered nanoparticles. *Environ. Sci. Pollut. Res.* 22, 1841–1853.
- Apel, K., Hirt, H., 2004. Reactive oxygen species: metabolism, oxidative stress, and signal transduction. *Annu. Rev. Plant Biol.* 55, 373–399.
- Baccouch, S., Chaoui, A., Ferjani, E. El, 2006. Nickel toxicity induces oxidative damage in zeamays roots. *J. Plant Nutr.* 24, 1085–1097.
- Benzie, I.F.F., Strain, J.J., 1999. [2] Ferric reducing/antioxidant power assay: Direct measure of total antioxidant activity of biological fluids and modified version for simultaneous measurement of total antioxidant power and ascorbic acid concentration, in: *Methods in Enzymology*. Elsevier, pp. 15–27.
- Berridge, M. V, Herst, P.M., Tan, A.S., 2005. Tetrazolium dyes as tools in cell biology: new insights into their cellular reduction. *Biotechnol. Annu. Rev.* 11, 127–152.
- Blokhina, O., Virolainen, E., Fagerstedt, K. V., 2003. Antioxidants, oxidative damage and oxygen deprivation stress: A review. *Ann. Bot.* 91, 179–194. doi:10.1093/aob/mcf118
- Brown, P.H., Welch, R.M., Cary, E.E., 1987. Nickel: A micronutrient essential for higher plants. *Plant Physiol.* 85, 801–803.
- Casida Jr, L.E., Klein, D.A., Santoro, T., 1964. Soil dehydrogenase activity. *Soil Sci.* 98, 371–376.
- Costa, A., Drago, I., Behera, S., Zottini, M., Pizzo, P., Schroeder, J.I., Pozzan, T., Schiavo, F. Lo, 2010. H₂O₂ in plant peroxisomes: an in vivo analysis uncovers a Ca²⁺-dependent scavenging system. *Plant J.* 62, 760–772.
- Dixit, V., Pandey, V., Shyam, R., 2001. Differential antioxidative responses to cadmium in roots and leaves of pea (*Pisum sativum* L. cv. Azad). *J. Exp. Bot.* 52, 1101–1109.

- Du, W., Gardea-Torresdey, J.L., Xie, Y., Yin, Y., Zhu, J., Zhang, X., Ji, R., Gu, K., Peralta-Videa, J.R., Guo, H., 2017. Elevated CO₂ levels modify TiO₂ nanoparticle effects on rice and soil microbial communities. *Sci. Total Environ.* 578, 408–416.
- Faisal, M., Saquib, Q., Alatar, A.A., Al-khedhairi, A.A., Hegazy, A.K., Musarrat, J., 2013. Phytotoxic hazards of NiO-nanoparticles in tomato : A study on mechanism of cell death. *J. Hazard. Mater.* 250–251, 318–332. doi:10.1016/j.jhazmat.2013.01.063
- Feelisch, M., Noack, E.A., 1987. Correlation between nitric oxide formation during degradation of organic nitrates and activation of guanylate cyclase. *Eur. J. Pharmacol.* 139, 19–30.
- Feierabend, J., Beevers, H., 1972. Developmental studies on microbodies in wheat leaves: I. Conditions influencing enzyme development. *Plant Physiol.* 49, 28–32.
- Foyer, C., Noctor, G., 2000. Oxygen processing in photosynthesis: regulation and signaling. *New Phytol.* 146, 359–388.
- Foyer, C.H., 1993. Ascorbic acid, in: Alscher, RG & Hess, J. (Ed.), *Antioxidants in Higher Plants*. CRC, Boca Raton, FL, USA, pp. 31–58.
- Foyer, C.H., Noctor, G., 2009. Redox Regulation in Photosynthetic Organisms. *Antioxidants redox Signal.* 11, 861–905. doi:10.1089/ars.2008.2177
- Gajewska, E., Skłodowska, M., 2007. Effect of nickel on ROS content and antioxidative enzyme activities in wheat leaves. *Biometals* 20, 27–36.
- Gajewska, E., Skłodowska, M., Slaba, M., Mazur, J., 2006. Effect of nickel on antioxidative enzyme activities, proline and chlorophyll contents in wheat shoots. *Biol. Plant.* 50, 653–659.
- Guo, B., Dai, S., Wang, R., Guo, J., Ding, Y., Xu, Y., 2015. Combined effects of elevated CO₂ and Cd-contaminated soil on the growth, gas exchange, antioxidant defense, and Cd accumulation of poplars and willows. *Environ. Exp. Bot.* 115, 1–10. doi:10.1016/j.envexpbot.2015.02.002
- Guo, H., Zhu, J., Zhou, H., Sun, Y., Yin, Y., Pei, D., Ji, R., Wu, J., Wang, X., 2011. Elevated CO₂ levels affects the concentrations of copper and cadmium in crops grown in soil contaminated with heavy metals under fully open-air field conditions. *Environ. Sci. Technol.* 45, 6997–7003. doi:10.1021/es2001584
- Hermes, D.A., Mattson, W.J., 1992. The dilemma of plants: to grow or defend. *Q. Rev. Biol.* 67, 283–335.
- Hodges, D.M., DeLong, J.M., Forney, C.F., Prange, R.K., 1999. Improving the thiobarbituric acid-reactive-substances assay for estimating lipid peroxidation in plant tissues containing anthocyanin and other interfering compounds. *Planta* 207, 604–611. doi:10.1007/s004250050524
- IPCC, 2013. *Climate Change 2013: The Physical Science Basis. Contribution of Working Group I to the Fifth Assessment Report of the Intergovernmental Panel on Climate Change.*

Cambridge University Press, New York..

- Jia, X., Liu, T., Zhao, Y., He, Y., Yang, M., 2016a. Elevated atmospheric CO₂ affected photosynthetic products in wheat seedlings and biological activity in rhizosphere soil under cadmium stress. *Environ. Sci. Pollut. Res.* 23, 514–526. doi:10.1007/s11356-015-5288-7
- Jia, X., Zhao, Y., Liu, T., Huang, S., 2016b. Elevated CO₂ affects secondary metabolites in *Robinia pseudoacacia* L. seedlings in Cd- and Pb-contaminated soils. *Chemosphere* 160, 199–207. doi:10.1016/j.chemosphere.2016.06.089
- Jia, Y., Tang, S., Wang, R., Ju, X., Ding, Y., Tu, S., Smith, D.L., 2010. Effects of elevated CO₂ on growth, photosynthesis, elemental composition, antioxidant level, and phytochelatin concentration in *Lolium mutiforum* and *Lolium perenne* under Cd stress. *J. Hazard. Mater.* 180, 384–394. doi:10.1016/j.jhazmat.2010.04.043
- Jiang, F., Shen, Y., Ma, C., Zhang, X., Cao, W., Rui, Y., 2017. Effects of TiO₂ nanoparticles on wheat (*Triticum aestivum* L.) seedlings cultivated under super-elevated and normal CO₂ conditions. *PLoS One* 12, e0178088. doi:10.1371/journal.pone.0178088
- Katsumiti, A., Arostegui, I., Oron, M., Gilliland, D., Valsami-Jones, E., Cajaraville, M.P., 2016. Cytotoxicity of Au, ZnO and SiO₂ NPs using in vitro assays with mussel hemocytes and gill cells: relevance of size, shape and additives. *Nanotoxicology* 10, 185–193.
- Kebeish, R., Niessen, M., Thiruveedhi, K., Bari, R., Hirsch, H.-J., Rosenkranz, R., Stähler, N., Schönfeld, B., Kreuzaler, F., Peterhänsel, C., 2007. Chloroplastic photorespiratory bypass increases photosynthesis and biomass production in *Arabidopsis thaliana*. *Nat. Biotechnol.* 25, 593.
- Kim, H.-J., Lee, J.-H., 2014. Highly sensitive and selective gas sensors using p-type oxide semiconductors: Overview. *Sensors Actuators B Chem.* 192, 607–627.
- Kooti, M., Jorfi, M., 2009. Synthesis and characterization of nanosized NiO₂ and NiO using Triton®X-100. *Open Chem.* 7, 155–158.
- Levine, R.L., Williams, J.A., Stadtman, E.P., Shacter, E., 1994. Carbonyl assays for determination of oxidatively modified proteins, in: *Methods in Enzymology*. Elsevier, pp. 346–357.
- Li, Z., Tang, S., Deng, X., Wang, R., Song, Z., 2010. Contrasting effects of elevated CO₂ on Cu and Cd uptake by different rice varieties grown on contaminated soils with two levels of metals: Implication for phytoextraction and food safety. *J. Hazard. Mater.* 177, 352–361. doi:10.1016/j.jhazmat.2009.12.039
- Meena, R., Kajal, K., Paulraj, R., 2015. Cytotoxic and genotoxic effects of titanium dioxide nanoparticles in testicular cells of male wistar rat. *Appl. Biochem. Biotechnol.* 175, 825–840.
- Misra, B.B., Chen, S., 2015. Advances in understanding CO₂ responsive plant metabolomes in the era of climate change. *Metabolomics* 11, 1478–1491. doi:10.1007/s11306-015-0825-4

- Mohamed, M.S.M., Saleh, A.M., Abdel-Farid, I.B., El-Naggar, S.A., 2017. Growth, hydrolases and ultrastructure of *Fusarium oxysporum* as affected by phenolic rich extracts from several xerophytic plants. *Pestic. Biochem. Physiol.* 141, 57–64.
- Murphy, M.E., Noack, E., 1994. Nitric oxide assay using hemoglobin method, in: *Methods in Enzymology*. Elsevier, pp. 240–250.
- Noguchi, K., Watanabe, C.K., Terashima, I., 2015. Effects of Elevated Atmospheric CO₂ on Primary Metabolite Levels in *Arabidopsis thaliana* Col-0 Leaves: An Examination of Metabolome Data. *Plant Cell Physiol.* 56, 2069–2078.
- Nowack, B., Bucheli, T.D., 2007. Occurrence, behavior and effects of nanoparticles in the environment. *Environ. Pollut.* 150, 5–22.
- Nunes-Nesi, A., Fernie, A.R., Stitt, M., 2010. Metabolic and signaling aspects underpinning the regulation of plant carbon nitrogen interactions. *Mol. Plant* 3, 973–996.
- OECD, 2006. Test No. 208: Terrestrial plant test: Seedling emergence and seedling growth test. OECD Guidelines for the Testing of Chemicals, Section, 2. OECD Publ. Paris.
- Pandey, V.K., Gopal, R., 2010. Nickel Toxicity Effects on Growth and Metabolism of Eggplant Nickel Toxicity Effects on Growth and Metabolism. *Int. J. Veg. Sci.* 16, 351–360.
- Pandolfini, T., Gabbrielli, R., Comparini, C., 1992. Nickel toxicity and peroxidase activity in seedlings of *Triticum aestivum* L. *Plant. Cell Environ.* 15, 719–725.
- Pérez-López, U., Robredo, A., Lacuesta, M., Sgherri, C., Muñoz-Rueda, A., Navari-Izzo, F., Mena-Petite, A., 2009. The oxidative stress caused by salinity in two barley cultivars is mitigated by elevated CO₂. *Physiol. Plant.* 135, 29–42.
- Pietrini, F., Bianconi, D., Massacci, A., Iannelli, M.A., 2016. Combined effects of elevated CO₂ and Cd-contaminated water on growth, photosynthetic response, Cd accumulation and thiolic components status in *Lemna minor* L. *J. Hazard. Mater.* 309, 77–86.
- Quan, L.-J., Zhang, B., Shi, W.-W., Li, H.-Y., 2008. Hydrogen peroxide in plants: a versatile molecule of the reactive oxygen species network. *J. Integr. Plant Biol.* 50, 2–18.
- Rodrigues, A., Pigatto, J., Barcelos, D.Q., Rones, C., Souza, W. De, Ferreira, E., Aparecido, L., Lisboa, M., Mateus, J., Santini, K., José, M., Furlani, E., Campos, M., Alexandre, P., Figueiredo, M. De, Lavres, J., 2017. A glimpse into the physiological, biochemical and nutritional status of soybean plants under Ni-stress conditions. *Environ. Exp. Bot.* 144, 76–87. doi:10.1016/j.envexpbot.2017.10.006
- Sager, T., Wolfarth, M., Keane, M., Porter, D., Castranova, V., Holian, A., 2016. Effects of nickel-oxide nanoparticle pre-exposure dispersion status on bioactivity in the mouse lung. *Nanotoxicology* 10, 151–161.
- Salimi, A., Sharifi, E., Noorbakhsh, A., Soltanian, S., 2007. Immobilization of glucose oxidase on electrodeposited nickel oxide nanoparticles: direct electron transfer and electrocatalytic activity. *Biosens. Bioelectron.* 22, 3146–3153.

- Savolainen, K., Alenius, H., Norppa, H., Pylkkänen, L., Tuomi, T., Kasper, G., 2010. Risk assessment of engineered nanomaterials and nanotechnologies—a review. *Toxicology* 269, 92–104.
- Schwitzguebel, J.-P., Siegenthaler, P.-A., 1984. Purification of peroxisomes and mitochondria from spinach leaf by Percoll gradient centrifugation. *Plant Physiol.* 75, 670–674.
- Seregin, I. V., Kozhevnikova, A.D., 2006. Physiological role of nickel and its toxic effects on higher plants. *Russ. J. Plant Physiol.* 53, 257–277.
- Seth, C.S., Remans, T., Keunen, E., Jozefczak, M., Gielen, H., Opdenakker, K., Weyens, N., Vangronsveld, J., Cuypers, A., 2012. Phytoextraction of toxic metals: a central role for glutathione. *Plant. Cell Environ.* 35, 334–346.
- Soares, C., Branco-neves, S., Sousa, A. De, Azenha, M., Cunha, A., Pereira, R., Fidalgo, F., 2018. SiO₂ nanomaterial as a tool to improve *Hordeum vulgare* L. tolerance to nano-NiO stress. *Sci. Total Environ.* 622–623, 517–525. doi:10.1016/j.scitotenv.2017.12.002
- Soares, C., de Sousa, A., Pinto, A., Azenha, M., Teixeira, J., Azevedo, R.A., Fidalgo, F., 2016. Effect of 24-epibrassinolide on ROS content, antioxidant system, lipid peroxidation and Ni uptake in *Solanum nigrum* L. under Ni stress.pdf. *Environ. Exp. Bot.* 122, 115–125.
- Srivastava, G., Kumar, S., Dubey, G., Mishra, V., Prasad, S.M., 2012. Nickel and ultraviolet-B stresses induce differential growth and photosynthetic responses in *Pisum sativum* L. Seedlings. *Biol. Trace Elem. Res.* 149, 86–96. doi:10.1007/s12011-012-9406-9
- Torabifard, M., Arjmandi, R., Rashidi, A., Nouri, J., Mohammadfam, I., 2018. Inherent health and environmental risk assessment of nanostructured metal oxide production processes. *Environ. Monit. Assess.* 190, 73.
- Tuba, Z., Raschi, A., Lanini, G.M., Nagy, Z., Helyes, L., Vodnik, D., Di Toppi, L.S., 2003. Plant response to elevated carbon dioxide, in: *Abiotic Stresses in Plants*. Springer, pp. 157–204.
- Uruç Parlak, K., 2016. Effect of nickel on growth and biochemical characteristics of wheat (*Triticum aestivum* L.) seedlings. *NJAS - Wageningen J. Life Sci.* 76, 1–5. doi:10.1016/j.njas.2012.07.001
- Watanabe, C.K., Sato, S., Yanagisawa, S., Uesono, Y., Terashima, I., Noguchi, K., 2014. Effects of elevated CO₂ on levels of primary metabolites and transcripts of genes encoding respiratory enzymes and their diurnal patterns in *Arabidopsis thaliana*: Possible relationships with respiratory rates. *Plant Cell Physiol.* 55, 341–357.
- Yadav, R.C., Patra, A.K., Purakayastha, T.J., Bhattacharyya, R., Singh, R., 2014. Response of rice plant to application of nanoparticles of Fe and Zn at elevated CO₂: A Hydroponic experiment under phytotron. *Int. J. Bio-Resource Stress Manag.* 5.
- Yadav, S.K., 2010. Heavy metals toxicity in plants: An overview on the role of glutathione and phytochelatin in heavy metal stress tolerance of plants. *South African J. Bot.* 76, 167–179.
- Yusuf, M., Fariduddin, Q., Hayat, S., Ahmad, A., 2011. Nickel: an overview of uptake,

essentiality and toxicity in plants. *Bull. Environ. Contam. Toxicol.* 86, 1–17.

Zhu, X.-J., Hu, J., Dai, H.-L., Ding, L., Jiang, L., 2012. Reduced graphene oxide and nanosheet-based nickel oxide microsphere composite as an anode material for lithium ion battery. *Electrochim. Acta* 64, 23–28.

Zinta, G., Abdelgawad, H., Domagalska, M.A., Vergauwen, L., Knapen, D., Nijs, I., Janssens, I.A., Beemster, G.T.S., Asard, H., 2014. Physiological, biochemical, and genome-wide transcriptional analysis reveals that elevated CO₂ mitigates the impact of combined heat wave and drought stress in *Arabidopsis thaliana* at multiple organizational levels. *Glob. Chang. Biol.* 20, 3670–3685.

ACCEPTED MANUSCRIPT

Figure Captions

Figure 1. Characterization of NiO-nanoparticles using scanning electron microscope (SEM) (a), UV-VIZ spectroscopy (b) and Fourier transform infrared spectroscopy (FTIR, c).

Figure 2. Effect of NiO-nanoparticles (NiO-NPs), elevated CO₂ (eCO₂) and their combination (NiO-NPs+eCO₂) on the accumulation of oxidative stress markers, levels of molecular antioxidants and the activity of antioxidant enzymes in shoot (A) and root (B) of wheat. Each value is the mean of 3 independent replicates and vertical bars represent the standard error. Same lower-case letters on bars, in the same chart, indicate non-significant difference at the 0.05 probability level. MDA, malondialdehyde; NO, nitric oxide; TTC-DHA, triphenyl tetrazolium chloride–dehydrogenase activity; TAC, total antioxidant capacity; SOD, superoxide dismutase; APX, ascorbate peroxidase; CAT, catalase; POD, peroxidase; GPX, glutathione peroxidase; GST, glutathione S-transferase; ASC, reduced ascorbate; DHA, oxidized ascorbate; GSH, reduced glutathione; GSSG, oxidized glutathione; DHAR, dehydroascorbate reductase; MDHAR, monodehydroascorbate reductase; GR, glutathione reductase. Same lower-case letters on bars indicate no significant difference at the 0.05 probability level.

Figure 3. Heatmap for oxidative stress markers and antioxidant metabolites and enzymes in root and shoot of wheat grown under NiO-nanoparticles (NiO-NPs), elevated CO₂ (eCO₂) and their combination (NiO-NPs+eCO₂). MDA, malondialdehyde; NO, nitric oxide; TTC-DHA, triphenyl tetrazolium chloride–dehydrogenase activity; TAC, total antioxidant capacity; SOD, superoxide dismutase; APX, ascorbate peroxidase; CAT, catalase; POD, peroxidase; GPX, glutathione peroxidase; GST, glutathione S-transferase; ASC, reduced ascorbate; DHA, oxidized ascorbate; GSH, reduced glutathione; GSSG, oxidized glutathione; DHAR, dehydroascorbate reductase; MDHAR, monodehydroascorbate reductase; GR, glutathione reductase. The relative accumulation patterns are shown in the heatmap based on the average value (n = 3) for each parameter. Red and blue colors indicate lower and higher concentrations, respectively.

Figure 4. An overview of the impact of NiO-nanoparticles (NiO-NPs) on growth, physiology and redox homeostasis of wheat under ambient CO₂ (aCO₂) or elevated CO₂ (eCO₂). As compared with the control plant, +, = and – indicate positive, tolerant and negative impact, respectively. PODs, peroxidases; ASC, reduced ascorbate; DHA, oxidized ascorbate; GSH, reduced glutathione; GSSG, oxidized glutathione.

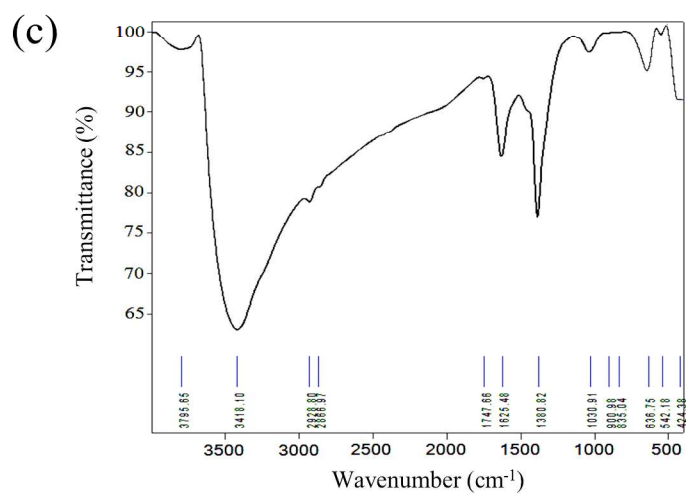
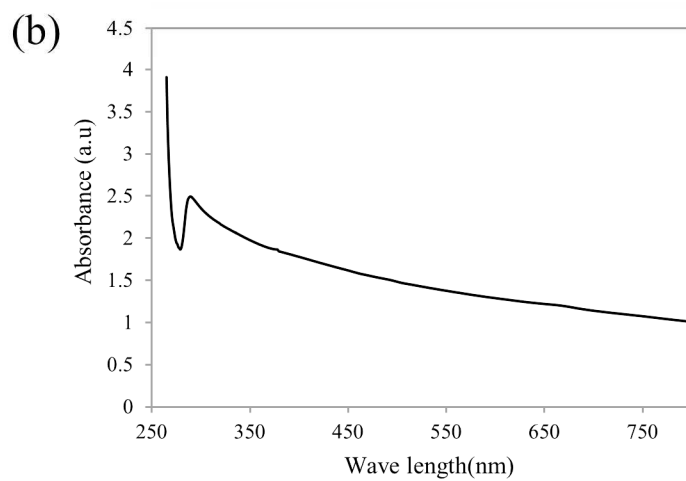
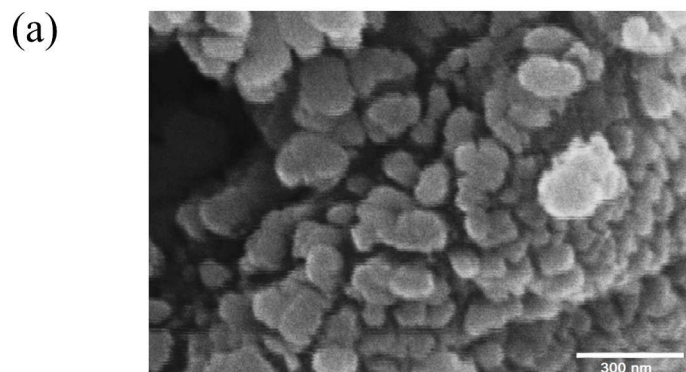
Table 1: Effect of NiO nanoparticles (NiO-NPs), elevated CO₂ (eCO₂) and their combination (NiO-NPs+eCO₂) on biomass production and accumulation of Ni ions in shoot and root of wheat. Values are mean \pm standard error of three independent replicates. Means followed by the same lower-case letter in a row do not differ significantly at the 0.05 probability level.

	Control	eCO ₂	NiO-NPs	NiO-NPs+eCO ₂
Fresh weight (g plant ⁻¹)				
Shoot	2.244 \pm 0.162c	2.899 \pm 0.109d	1.319 \pm 0.036a	1.999 \pm 0.101b
Root	0.365 \pm 0.026cd	0.401 \pm 0.018d	0.147 \pm 0.006a	0.247 \pm 0.012b
Total	2.610 \pm 0.180c	3.300 \pm 0.120d	1.465 \pm 0.040a	2.240 \pm 0.110b
Dry weight (g plant ⁻¹)				
Shoot	0.337 \pm 0.015c	0.422 \pm 0.010d	0.198 \pm 0.007a	0.294 \pm 0.015b
Root	0.050 \pm 0.003c	0.069 \pm 0.002d	0.024 \pm 0.001a	0.040 \pm 0.002b
Total	0.388 \pm 0.020c	0.491 \pm 0.010d	0.222 \pm 0.010a	0.334 \pm 0.020b
Ni accumulation (mg g ⁻¹ DW)				
Shoot	0.0039 \pm 0.001a	0.0037 \pm 0.001a	0.307 \pm 0.083b	0.292 \pm 0.039b
Root	0.0044 \pm 0.000a	0.0041 \pm 0.001a	1.806 \pm 0.155b	1.688 \pm 0.135b

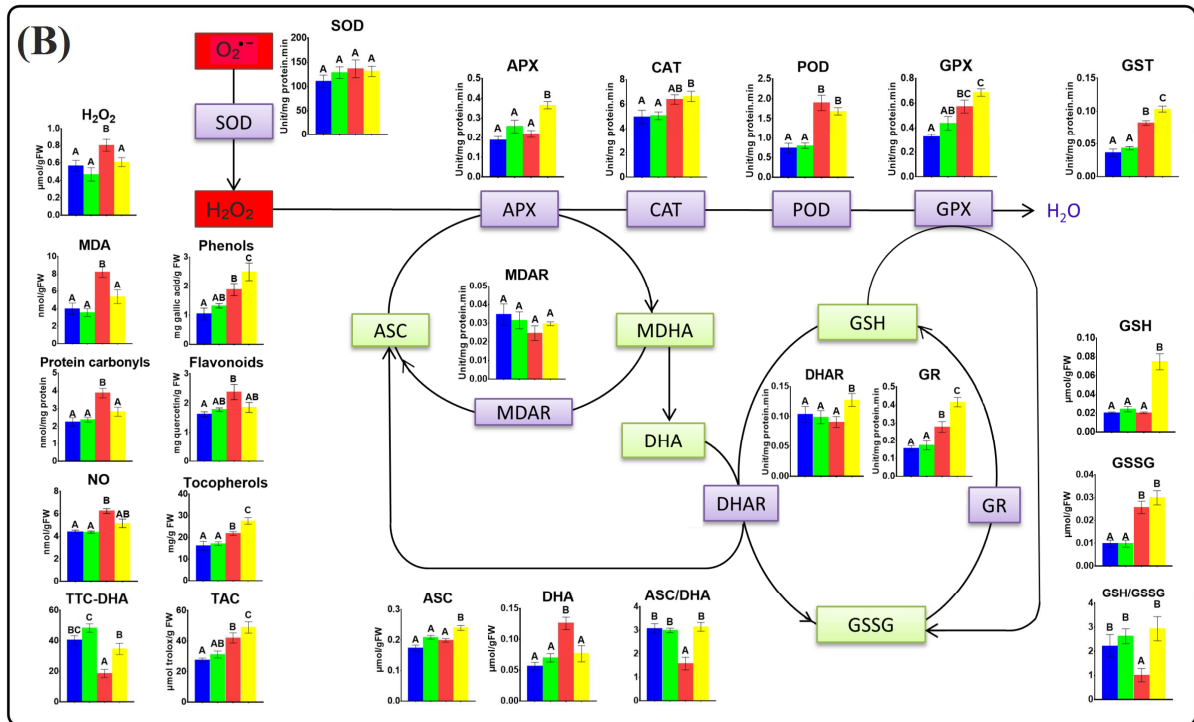
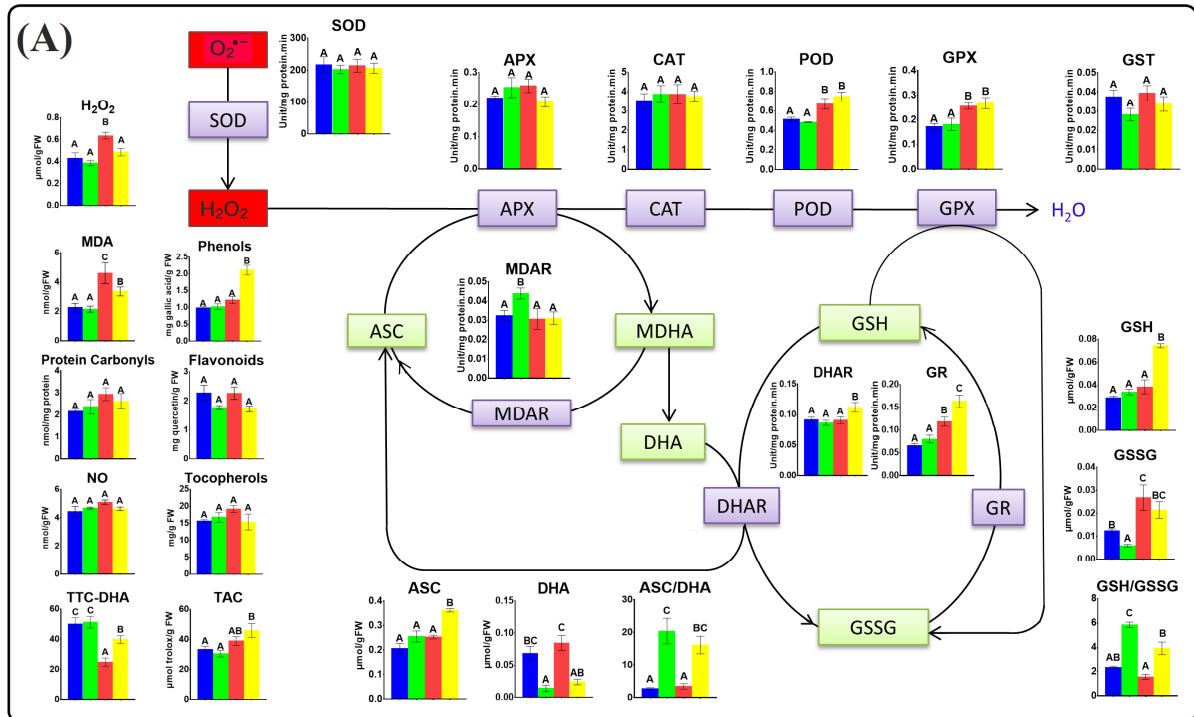
Table 2:

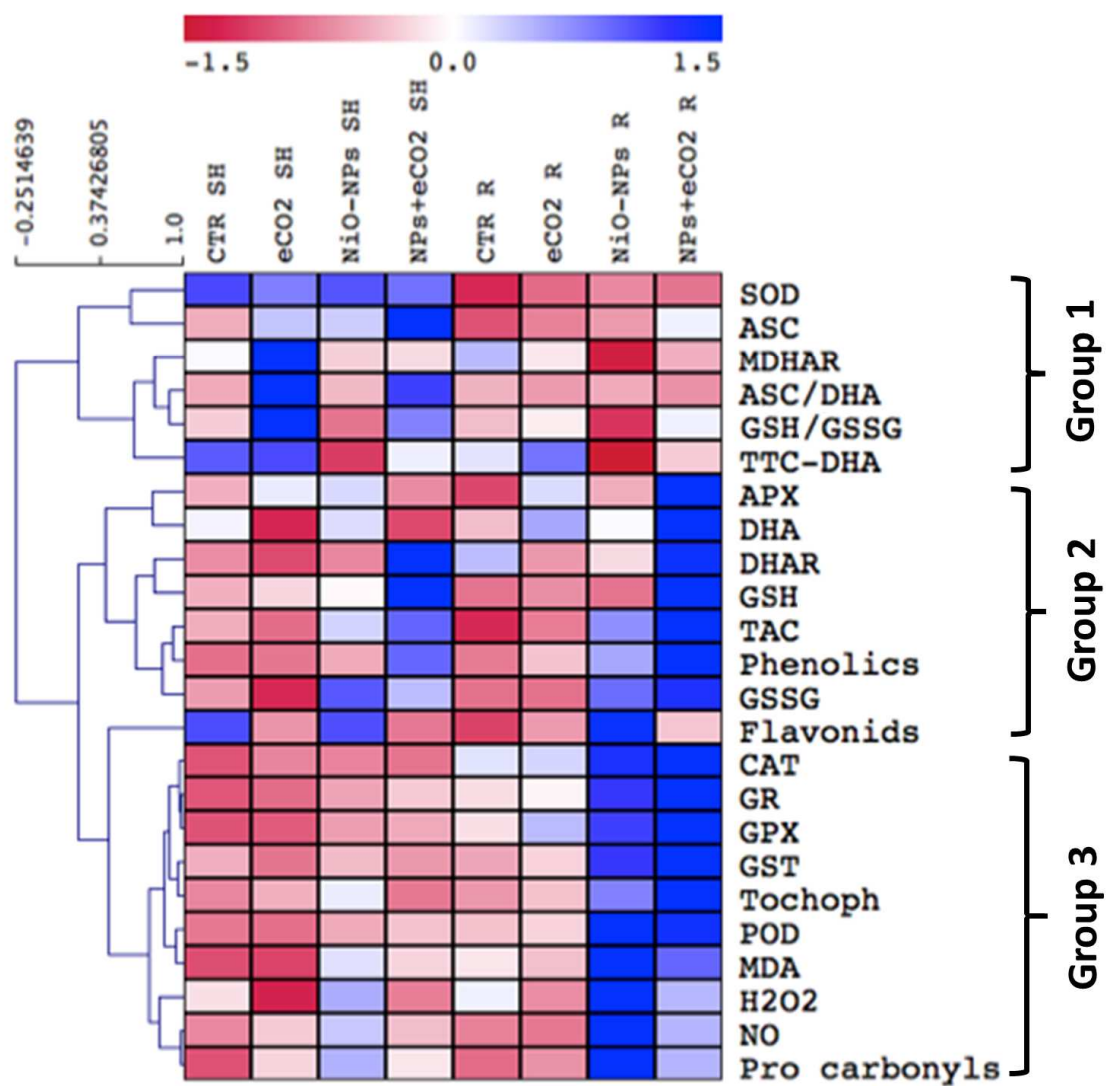
Effect of NiO nanoparticles (NiO-NPs), elevated CO₂ (eCO₂) and their combination (NiO-NPs+eCO₂) on photosynthesis and photorespiration related parameters in wheat. Values are mean \pm standard error of three independent replicates. Means followed by the same lower-case letter in a row do not differ significantly at the 0.05 probability level.

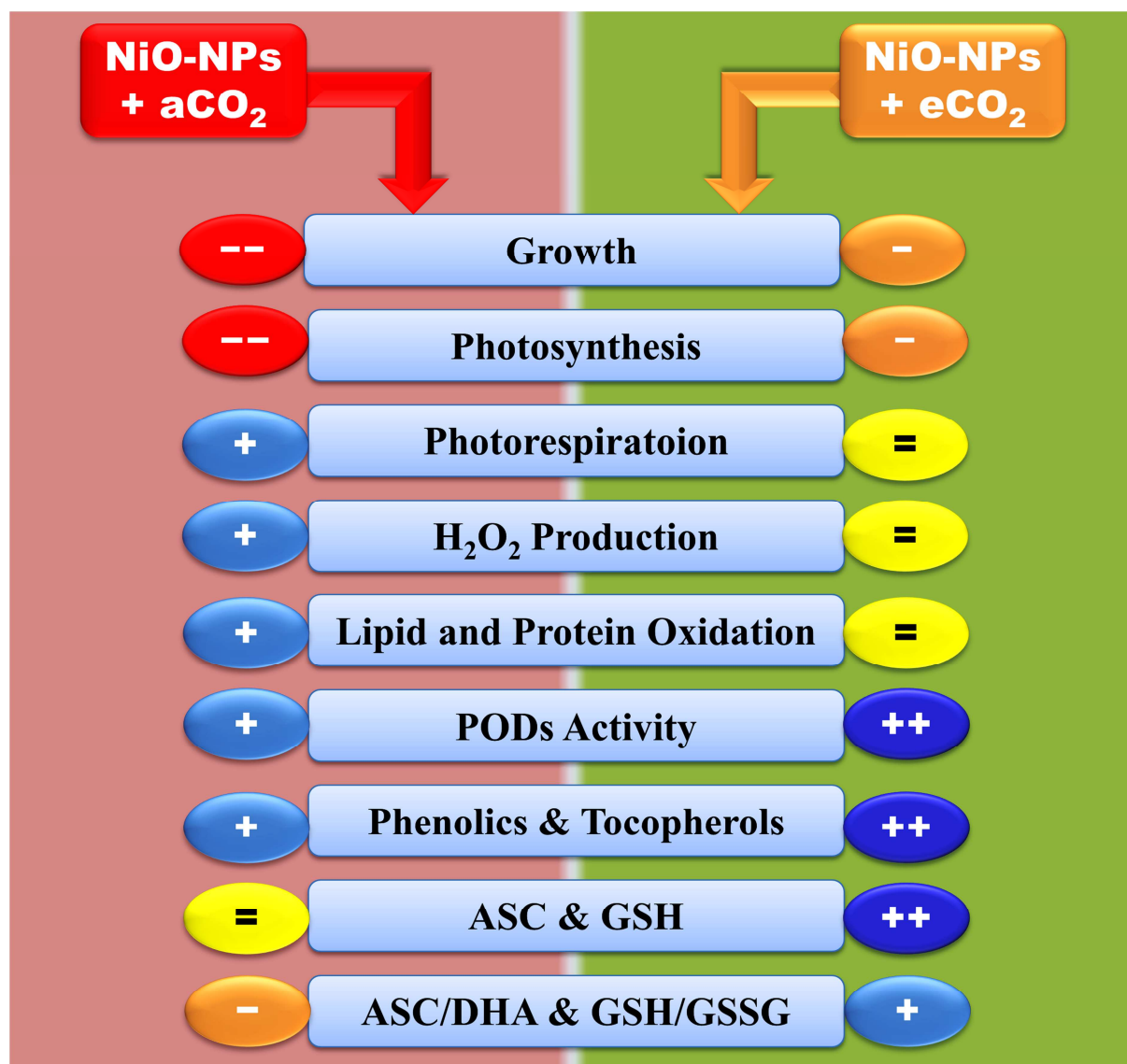
	Control	eCO ₂	NiO-NPs	NiO-NPs+eCO ₂
Photosynthesis related parameters				
Chlorophyll (mg g ⁻¹ FW)	0.15 \pm 0.02b	0.19 \pm 0.03b	0.05 \pm 0.00a	0.12 \pm 0.01b
Carotenoids (mg g ⁻¹ FW)	0.021 \pm 0.002a	0.018 \pm 0.003a	0.038 \pm 0.007b	0.027 \pm 0.003a
Rate of photosynthesis (μ mol CO ₂ m ⁻² s ⁻¹)	7.29 \pm 0.66c	9.45 \pm 1.04d	3.24 \pm 0.47a	5.94 \pm 0.64b
Chlorophyll Fluorescence (F _v /F _m)	0.80 \pm 0.00c	0.80 \pm 0.01c	0.65 \pm 0.01a	0.71 \pm 0.01b
Rubisco activity (nmol 3-PGA mg protein ⁻¹ min ⁻¹)	71.88 \pm 9.25b	76.46 \pm 3.33b	31.61 \pm 2.77a	74.70 \pm 11.43b
Stomatal conductance (mmol m ⁻² s ⁻¹)	129.98 \pm 5.13b	119.72 \pm 9.37b	101.23 \pm 5.84a	113.77 \pm 6.22ab
Starch (mg g ⁻¹ FW)	6.35 \pm 0.73b	7.71 \pm 0.69c	3.48 \pm 0.41a	5.87 \pm 0.24b
Photorespiration related parameters				
GO (unit/mg protein.min)	1.00 \pm 0.12a	0.87 \pm 0.05a	2.45 \pm 0.12b	1.22 \pm 0.08a
HPR (unit/mg protein.min)	2.06 \pm 0.29a	1.96 \pm 0.21a	4.01 \pm 0.26b	2.89 \pm 0.20a
GLY/SER	0.56 \pm 0.02a	0.52 \pm 0.05a	0.72 \pm 0.04b	0.59 \pm 0.05a



Control eCO₂ NiO-NPs NiO-NPs+eCO₂







Highlights

- NiO-NPs alone induced severe growth and oxidative damage in wheat.
- eCO₂ did not affect the accumulation and translocation of Ni in wheat, but antagonizes its phytotoxicity.
- eCO₂ promoted photosynthetic reactions and thus mitigated growth reduction in NiO-NPs treated wheat.
- eCO₂ reduced ROS induced cellular damage and maintained redox balance under NiO-NPs stress.
- ROS content were reduced at production level, via decreased photorespiration and at detoxification level by improved antioxidant defenses.
- Root was more responsive to imposed treatments and used several strategies to overcome stress impact.